

Application of Neural Networks to Load Frequency Control in Power Systems with Four Control Areas

Aldi Mucka¹, Astrit Bardhi², Denis Qirollari³

^{1,2}Polytechnic University of Tirana, Faculty of Electrical Engineering,
Bul. "Dëshmorët e Kombit" Square "Nënë Tereza", No. 4, Tirana, Albania

³National Grid US, 40 Sylvan Road, Waltham, MA, USA 02451

Abstract: Rapid population growth and technological development is a 21st century phenomenon. This phenomenon eventually increases the demand for electricity and its supply reliability. Power systems are complex networks consisting of generation, transmission and distribution of electricity to customers over a large geographical area. Power systems are interconnected to enable a secure and economical supply. Automatic Generation Control (AGC) or Load Frequency Control (LFC) is a very important subject in power systems for a reliable and quality of electricity supply to customer. Load Frequency Control helps to reduce deviations during transient processes by moving the error to zero value in steady state. The main objective of AGC in interconnected systems is to maintain the frequency at nominal values of the desired generation power output. There are various control techniques that have been applied to power and frequency control problems. The PI controller is among the simplest to implement but the set-up time is relatively large and causes a lot of oscillations in the frequency response. The best alternative to the PI controller is the widely used Fuzzy logic controller. However, this controller has its limitations as it has good dynamics only when defining the correct number of pointer functions. To enable an even better power and frequency tuning the controller with artificial neural networks (ANN) has found great use because it has faster control than other types and can improve transient response through training/learning procedure. This paper addresses the performance evaluation of the ANN controller in controlling power and frequency signals in four area interconnected system with a combination of thermal – thermal, hydro – thermal and hydro – hydro generation. It analyzes the performance of frequency response. The performance is estimated by comparing the result of PID controller with ANN controller.

Keywords: Load Frequency Control, Power System, ANN Controller

1. Introduction

Automatic Load-Frequency control helps to reduce deviations during transient processes by moving the error to zero value in steady state. For a successful operation of the interconnected power system the total generation must be equal to the total power demand including the system losses. A casual change of load in a control zone of an interconnected power system causes the frequency deviation from the nominal value. The main objective of AGC in interconnected systems is to maintain the frequency at nominal values of the desired generation power output. There are various control techniques that have been applied to power and frequency control problems. The PI controller is among the simplest to implement but the set-up time is relatively large and causes a lot of oscillations in the frequency response. The best alternative to the PI controller is the widely used Fuzzy logic controller. However, this controller has its limitations as it has good dynamics only when defining the correct number of pointer functions. To enable an even better power and frequency tuning the controller with artificial neural networks (ANN) has found great use because it has faster control than other types and can improve transient response through training/learning procedure.

This paper treats power system model simulations with four areas interconnected. The model is created and run in Simulink-MATLAB program. Model is run for two cases, the Case where controllers in the model are PID, and the case where the controllers are neural ANN. For each area is studied a system disturbance in the value of 0.02 p.u. or 40

MW. From simulation result are defined the frequency response, tie line active power difference, maximum deviation value of frequency and active power as well the graphic simulation the stand state error value. These values are compared for the respective models, zones and cases to see which type of controller gives the best performance in power frequency regulation of the power system.

2. Mathematic Models of the Power System Elements

2.1 Introduction

The first step in the design of control systems and analysis is based in mathematical modeling of all power system elements. The two most commonly used methodologies are the transmitting function method and the variable of the state. Method variables of state can be applied to describe in the same time the Linear and non-linear systems. To use the transmitting function and linear equations of state, the system must first be linearized. It is required to make approaches to the mathematical linearized equations that describe the system and so is obtained the transfer function model for the components to be checked.

2.2 Generator model

A small disturbance applied in the motion equation of a synchronous machine we get:

$$\frac{2H}{\omega_s} \frac{d^2 \Delta \delta}{dt^2} = \Delta P_m - \Delta P_e \quad (1)$$

Or the correlation with the speed change, if the speed is expressed in per unit, we get

$$\frac{d\Delta\omega}{dt} = \frac{1}{2H} (\Delta P_m - \Delta P_e) \quad (2)$$

Applying Laplace transformation, we get the above correlation and it is represented by the following block-diagram.

$$\Delta\Omega(s) = \frac{1}{2Hs} (\Delta P_m(s) - \Delta P_e(s)) \quad (3)$$

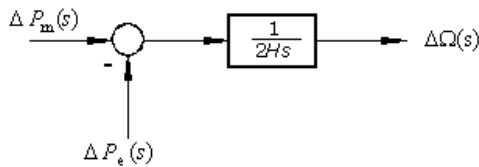


Figure 1: Generator block diagram

2.3 Load modeling

The Power System load comprises from various electrical equipment. For such as active loads such as lighting and heat, electrical power does not depend on frequency. In the case of motor loads, such as pumps and fans, electrical power varies with frequency due to the change in rotor speed. This change is subject of speed-load ratio characteristics. This characteristic can be expressed as:

$$\Delta P_e = \Delta P_L + D \Delta\omega \quad (4)$$

The reduction coefficient expresses the percentage change of load for one percent of frequency change. For example, if the load changes 1% for a frequency change of 1%, then D = 1. By including the load pattern in the generator block-diagram it is obtained the following block diagram.

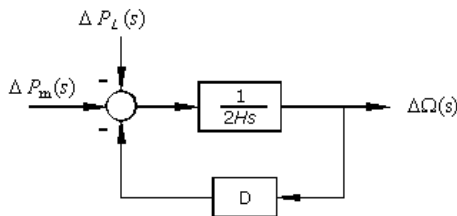


Figure 2: Load and Generator block diagram

This type of load model is used in the power system modeling with four zones. In the absence of the Governor, the system load change reaction is determined by both of inertia and reduction coefficients. For constant speeds, the deflection is such that the change in load is completely offset by the load fluctuation due to frequency sensitivity.

2.4 Primary Generator (thermal and hydro turbine)

The source of mechanical power, or otherwise known as the primary generator, can be a hydro or a steam turbine, which gets the power from the burning energy from coal, oil, gas, and nuclear resources. The turbine model associates the changes in mechanical power output to the changes in the steam valves position. The characteristics of different turbines may widely vary in their family range. The simplest

model of the primary generator for non - reheated steam turbines can be approximated with a time constant which leads us to the following transmission function:

$$G_T(s) = \frac{\Delta P_m(s)}{\Delta P_v(s)} = \frac{1}{1 + \tau_T s} \quad (5)$$

The block-diagram of a general turbine as is shown in Figure 4. The time coefficient is within the limits from 0.2 to 2.0 seconds.

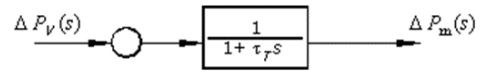


Figure 4: Block diagram of steam turbine non-reheated

Another type of steam turbine is called reheated steam turbine. The dynamic response of a steam turbine to the term of the output power change can be expressed as the change in steam valve opening. The relevant block-diagram of reheated steam turbine is shown in Figure 5. For simplicity study it is assumed that the turbine can be modeled with a single equivalent time coefficient is in the range of 0.2 to 2.5 seconds.

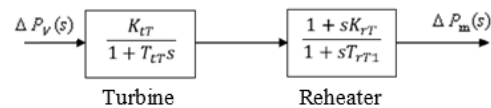


Figure 5: Block diagram of steam turbine with reheater

The modeling of the hydro turbine can be achieved from the turbine flow equations, the mechanical moment and the correlation of these equations to each other. The turbine flow equation states and the mechanical moment of the turbine is expressed as is show in Equation 6 and 7.

$$q_t = g + 0.5h \quad (6)$$

$$M = g + 1.5h \quad (7)$$

The gate “g” position and hash “h” are related to an impedance function

$$\frac{h}{q_t} = T_w s \quad (8)$$

The above three equations with numerical processing give the formula of the hydro turbine transmission function as is show in Equation 9.

$$\frac{M}{g} = \frac{1 - T_w s}{1 + 0.5T_w s} \quad (9)$$

2.5 Governor Model

When the machine (generator) load is increased instantaneously, the active power exceeds the amount of mechanical power at the inlet of the turbine. This power deficit is covered by the kinetic energy stored by the rotating masses. The decrease in kinetic energy causes the turbine speed to decrease and consequently will cause the frequency to drop. The difference in speed is detected by the speed control, which tends to adjust the valves at the inlet of the turbine in order to change the mechanical energy at the outlet of the turbine and keep the speed in another steady mode. Modern controllers use the electronic way to understand speed changes and often use the combination of electronic,

mechanical and hydraulic tools to make the necessary changes to the valve position. This type of controller is called a one-time controller (at constant speed), regulates valve entry at the point that drives the frequency back to its nominal value. If the output of the speed-sensitive mechanism is directly linked to the valve, the frequency is not likely to be brought to nominal value. The governor block diagram shown in Figure. 6 can be reduced as in the form shown in Figure 7. This type of speed controller is known as proportional controller with amplifier 1/R.

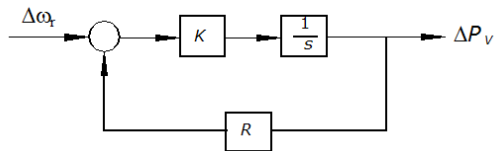


Figure 6: Block diagram of governor

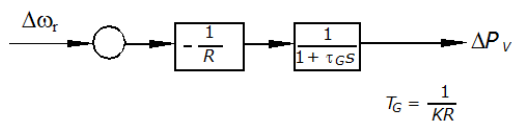


Figure 7: Block diagram of reduced governor

The slope of the curve R represents the drop of static characteristic. Controllers typically have a drop of (5-6) % from zero to nominal load. Drop represents the relationship between the speed change ($\Delta\omega$) or frequency change (Δf) and the change the power generated or the change of the position of the valve/gate. The transfer function of governor as is shown in Equation 10.

$$G_g(s) = \frac{1}{T_G s + 1} \tag{10}$$

2.6 Tie Line Model

In figure 8 are shown two power systems connected with one tie line. Both areas are represented by one equivalent generating unit interrelated with each other with a tie line with no losses, with the reactance X_{tie} of line. The areas are represented by a voltage source and an equivalent reactance. The active power transmitted over the tie line is:

$$P_{12} = \frac{|E_1||E_2|}{X_{12}} \sin \delta_{12} \tag{11}$$

Equation (11) may be linearized for a small deviation from the power flow nominal ΔP_{12} .

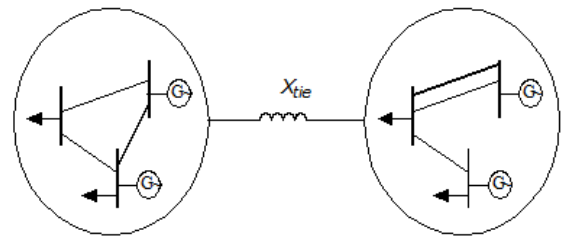
$$\Delta P_{12} = \left. \frac{dP_{12}}{d\delta_{12}} \right|_{\delta_{120}} \Delta \delta_{12} = P_s \Delta \delta_{12} \tag{12}$$

P_s presents to the slope of the power angle curve for a preliminary angle $\delta_{12} = \delta_1 - \delta_2$. This can be defined as the coefficient of synchronous power. Given this we get:

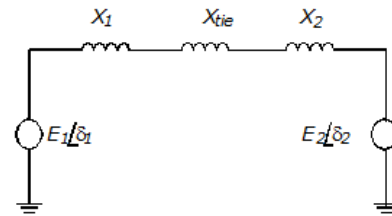
$$P_s = \left. \frac{dP_{12}}{d\delta_{12}} \right|_{\delta_{120}} = \frac{|E_1||E_2|}{X_{12}} \cos \Delta \delta_{120} \tag{13}$$

And the deviation of power in the interconnection line will take the form:

$$\Delta P_{12} = P_s (\Delta \delta_1 - \Delta \delta_2) \tag{14}$$



a)



b)

Figure 8: a) Two areas of interconnected power system
b) Equivalent circuit

3. Neural Networks and Narma -L2 Controller

3.1 Narma-L2 Neural Controller Architecture

An Artificial Neural Network is information that processes a pattern that is inspired by biological neural systems, such as the brain, that processes information. The key element of this model is the structure of this information processing system. It consists of many interconnected processing elements (neurons) that work together to solve specific problems. ANNs, like humans, learn through examples. An ANN is configured for a specific application, such as data sorting, through a learning process. Learning in biological systems involves regulation in the synaptic connections that exist between neurons. This is true for ANNs as well. Neuro-controller used for this analysis is known by two names: Feedback linearization control or Narma-L2 control. Work performed by this controller is a transformation of the non-linear dynamic system in linear dynamic system or otherwise in a reliable system. (Narendra and Mukopadhyay, 1997)

A Narma model accurately describes an unstable plant in the large interconnected plant network. There are two types of Narma controller known as Narma-L1 and Narma-L2. The peculiarity of these controllers is the fact that the controller impulse variable $u(k)$ at time k appears linearly in the equations that links input and output. This enables simpler numerical computation and only the use of static gradient methods. The proposed equations of the Narma-L2 model is presented below.

$$y(k+d) = f_0[y(k), (y(k-1), \dots, y(k-n+1)), u(k-1), \dots, u(k-n+1)] + g_0[y(k), y(k-1), \dots, y(k-n+1), u(k-1), \dots, u(k-n+1)]u(k) \tag{15}$$

The advantage of the Narma-L2 equation model is that it can be solved for input variables that cause the system output variables to follow the reference $y(k+d) = y_r(k+d)$. The result of the controller would be as follows:

$$y(k) = \frac{y_r(k+d) - f_0[y(k), (y(k-1), \dots, y(k-n+1), u(k-1), \dots, u(k-n+1))]}{g_0[y(k), (y(k-1), \dots, y(k-n+1), u(k-1), \dots, u(k-n+1))]} \quad (16)$$

The following figure shows the Narma-L2 controller used in linearizing the power system with four areas.

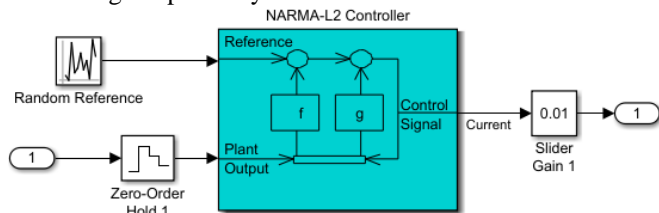


Figure 9: Narma - L2 controller used in power / frequency control of the system

After a series of modifications and errors, the ANN architecture enables the best performance. The data used in the Narma-L2 controller of the system are as follows:

ANN controller model data:

- Number of layers: 9
- Number of neurons in the hidden layer: 13
- Inputs: 3
- Outputs: 2

Plant Data with ANN controller

- Number of layers: 3
- Number of inputs: 4
- Number of neurons in the hidden layer: 10
- Number of outputs (output variables): 1
- Activation function: trainlm function
- Training Samples: 10000
- Training Epochs: 100

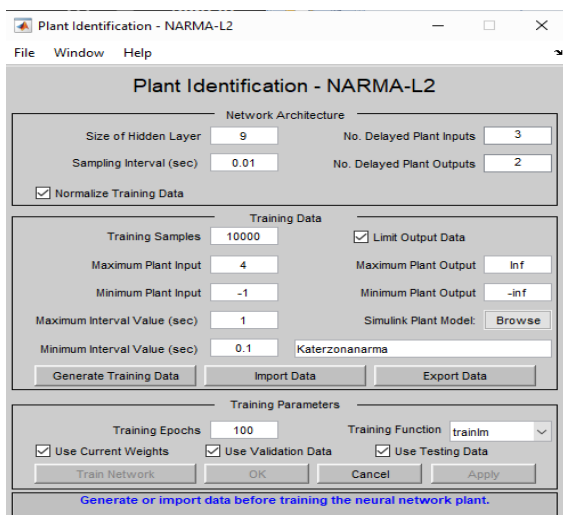


Figure 10: Narma-L2 Plant Identification

4. Plant Model

A four-area electric power system is considered as a test system is shown in Figure 11. In Figure 12 is show block diagram for area of interconnected areas build in Simulink work space.

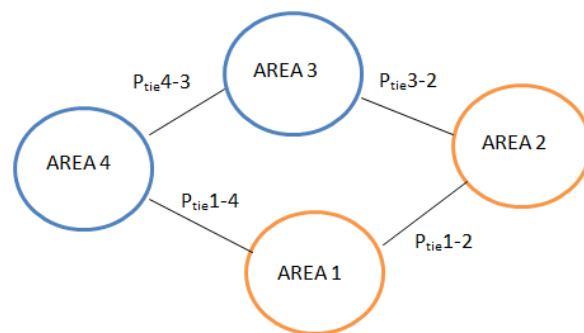


Figure 11: Four-area electric power system with interconnections

The four-zone power system is built of two zones with thermal power plants and two other zones with hydro power plants. They work in parallel at 50 Hz frequency and are interconnected with tie lines. Each control zone should contribute to power/frequency control to stabilize the system. The nomenclatures of the above equations are defined as follows:

- ΔPG = Generated power derivation, pu MW.
- ΔPD = Change in power demand, pu MW.
- ΔPC = Change in speed changer position (u), pu MW.
- Δf = Derivative in frequency, Hz.
- KP = Static gain of power system inertia dynamic block, Hz/pu MW.
- TP = Time constant of power system inertia dynamic block, sec.
- TG = Governor Time constant, sec.
- TT =Turbine (non -reheat type) time constant, sec.
- R = Speed regulation parameter, Hz/pu MW.

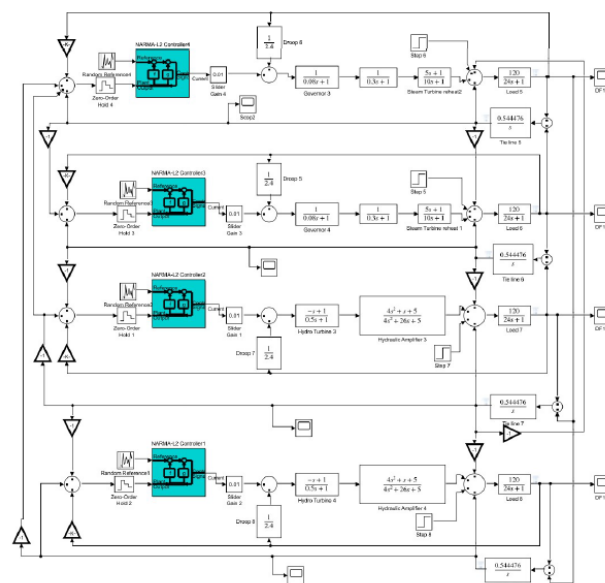


Figure 12: Block Diagram of four areas power system with Narma-L2 Plant controller in Simulink work space

5. Simulation Results

The typical values of system parameters for the nominal operating condition are as show in Table 1.

Table 1: System parameter data

Parameter	Value	Unit
R1, R2, R3, R4	2.4	Hz / p.u MW
B	0.00833	p.u MW / Hz
Kp1, Kp2, Kp3, Kp4	120	Hz / p.u MW
Tp1, Tp2, Tp3, Tp4	20	Second
b1, b2, b3 & b4	0.425	p.u MW / Hz
T0	0.0867	MW / radian
T12, T13, T23, T34	0.0867	MW / radian
Tg1 & Tg2	0,08	Second
Tt1 & Tt2	0.3	Second
Kr1 & Kr2	10	Second
Tw	0.10	Second
a12, a13, a23 & a34	1	-
April	2000	MW
Ptie, max	200	MW
f	60	Hz
ash	5	s
kp	16	hydro unit
ki	5	hydro unit
kd	4	hydro unit

The scheme of connecting the plant to the PID and ANN controllers is as show in Figure 12, and the component values obtained from the data of Table 1. A positive disturbance (load change) is presented in the system in zone 1 and 2 with a value 0.02 p.u or 40 MW and a disturbance in zone 3 and 4 of the same value. The total power generation per each zone is 2000 MW and the maximum interconnection line capacity is 200 MW.

Figure 13 show frequency response in thermal area 1 for both controllers. The ANN controllers reduce the stand state error to -0.01182 p.u. and the set frequency is 49.41Hz while in the case where the PID controller is used the error is reduced to -0.02793 p.u. and the set frequency is 48.6 Hz. Both controllers have a set time limit within 30 seconds respectively 22.4 sec for ANN case and 28.76 sec for PID case. The maximum values of the frequency deviations for the case of the scheme with ANN and PID controllers are -0.07318 p.u. and -0.09201 p.u.

Figure 14 show frequency response in hydro area 3 for both controllers. The frequency deviation in the case with PID controller is -0.02806 p.u. and the set frequency is 48,597 Hz and in the case of ANN frequency deviation is -0.01053 p.u. and the set frequency is 49.473 Hz. The time setting of ANN and PID case is respectively 31.75 sec and 22.78 sec. The maximum values of the frequency deviation in the case of PID and ANN controllers are -0.1022 p.u. and -0.09016 p.u.

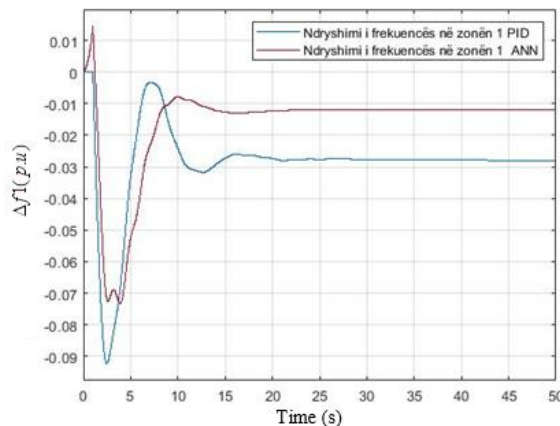


Figure 13: Frequency response in thermal Area 1 for PID and ANN controller

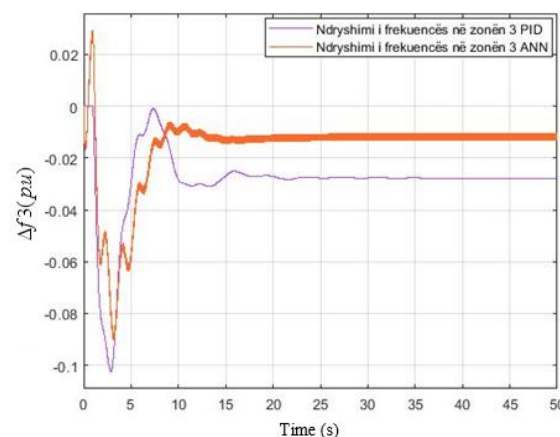


Figure 14: Frequency response in hydro Area 3 for PID and ANN controller

In figures 15 show the power deviation for tie line between area 2 and 3. Value for the case with PID and ANN controllers is +0.00734 p.u. and -1.036 * 10⁻⁵ p.u. The setting time for the PID and ANN case is 34.17sec and 32.09sec. The maximum value of active power deflection for the case with PID and ANN controller is 0.01325 p.u. and 0.00832 p.u. respectively.

Figures 16 show the power deviation for tie line between area 1 and 4. Value for the case with PID and ANN controllers is -0.0137 p.u. and 4.544*10⁻⁵ p.u. The setting time for the PID and ANN case is 41.63 sec and 37.52 sec. The maximum value of the active power deviation for the case with PID and ANN controller is -0.03601 p.u. and -0.01897 p.u.

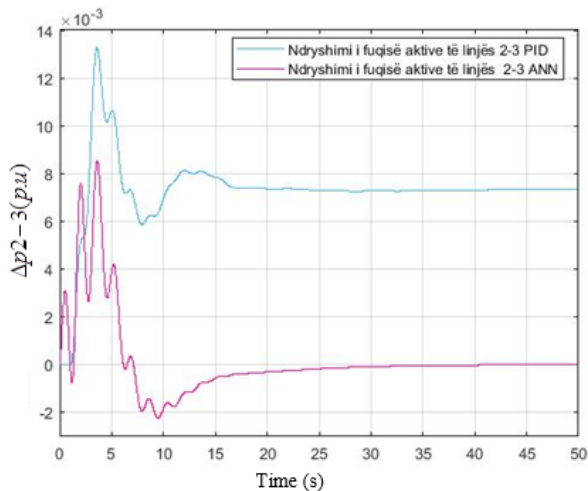


Figure 15: Power exchange response between Area 2 and 3

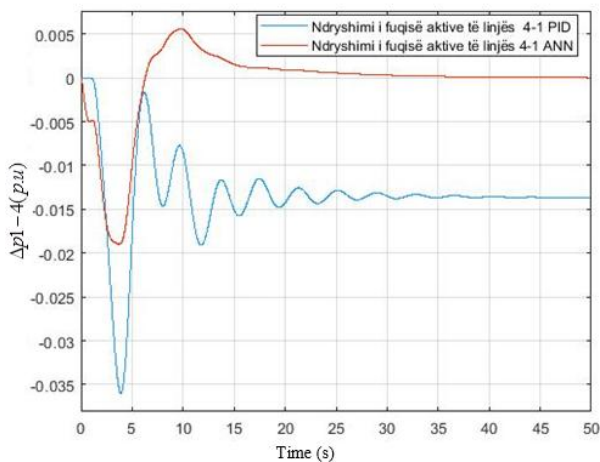


Figure 16: Power exchange response between Area 4 and 1

The above results obtained from the simulations show that the proposed use of neural controllers in the interconnected power system enables a better dynamic performance in terms of system power-frequency control by reducing static error and frequency deviation oscillations and of power in tie lines in any area with the combination of thermo and hydro in a relatively short time. The setting time and overshoot of response of the frequency and active power shift in the tie line are shown in Tables 2, 3 and 5 for the power system with four area model selected in both the PID and ANN controller cases.

Table 2: Comparison of time setting of frequency response by using ANN and PID controller

Controller	Area 1 (sec)	Area 2 (sec)	Area 3 (sec)	Area 4 (sec)
PID	28.76	31.98	31.75	36.8
ANN	22.4	22.87	22.78	23.03

Table 3: Comparison of time setting of power exchange response in tie line by using ANN and PID controller

Controller	Tie Line 1-2 (sec)	Tie line 2-3 (sec)	Tie line 3-4 (sec)	Tie Line 1-4 (sec)
PID	35.76	34.17	35.45	41.63
ANN	2:25	32.03	31.96	37.52

Table 4: Overshoot of frequency response by using ANN and PID controller

Controller	Area 1 (p.u)	Area 2 (p.u)	Area 3 (p.u)	Area 4 (p.u)
PID	-0.09201	-0.09077	-0.1022	-0.1233
ANN	-0.07318	-0.07259	-0.09016	-0.0856

Table 5: Overshoot of active power exchange response by using ANN and PID controller

Controller	Area 1 (p.u)	Area 2 (p.u)	Area 3 (p.u)	Area 4 (p.u)
PID	-0.00741	0.01325	-0.01088	-0.03601
ANN	-1.12x10^-18	0.00832	-0.00847	-0.01897

6. Conclusions

By using the ANN controller allows for shorter deployment time as well as lower active power and frequency deviations as well as less steady state error compared to the values obtained by using the PID controller in the system. PID controller systems are powered to maximize performance while ANN controller schemes are automatically powered by the controller training function. The parameters of the ANN controller are the minimum parameters with optimal performance. This means that if we increase the number of neurons and layers in the controller the values obtained during the simulation have further potential for improvement

References

- [1] C. Concordia and L.K. Kirchmayer, 'Tie line power and Frequency control of electric power systems,' Amer. Inst. Elect. Eng. Trans., Pt. II, Vol. 72, pp. 562-572, Jun. 1953.
- [2] IEEE PES Working Group, 'Hydraulic turbine and turbine control models for system dynamic Studies,' IEEE Trans. Power Syst., vol. PWRS-7, no. 1, pp. 167-174, Feb. 1992.
- [3] A. Khotanzad, R.A. Rohani, T.L. Lu, A. Abaye, M. Davis, and D.J. Maratukulam. ANNSTLF-A Neural-Network-Based Electric Load Forecasting System. IEEE Transactions on Neural Networks, 8:835-846, 1997.
- [4] M. Peng, N.F. Hubele, and G.G. Karady. Advancement in the Application of Neural Networks for Short-Term Load Forecasting. IEEE Transactions on Power Systems, 7:250-257, 1992.
- [5] R. Francis, Dr. I. A. Chidambaram , Automatic Generation Control for an Interconnected Reheat Thermal Power Systems Using Wavelet Neural Network Controller, International Journal of Emerging Technology and Advanced Engineering Website: www.ijetae.com (ISSN 2250-2459, Volume 2, Issue 4, April 2012)
- [6] A.D.Papalexopoulos, S. Hao, and T.M. Peng. An Implementation of a Neural Network Based Load Forecasting Model for the EMS. IEEE Transactions on Power Systems, 9:1956-1962, 1994.

Author Profile



Aldi Mucka received the B.S. and M.S. degrees in Electrical Engineering from Faculty of Electrical Engineering of Polytechnic of Tirana in 2008 and 2010, respectively. From 2010 he works as lector in Department of Power Systems in Faculty of Electrical Engineering. During this time he has get deep study in field of control and operation of electrical power system. He now is work as first Lector at Department of Power Systems.



Astrit Bardhi received the M.S. and Ph.D. degrees in Electrical Engineering from Faculty of Electrical Engineering of Polytechnic of Tirana in 2002 and 2011, respectively. From 2006, he works as lector in Department of Automation of Industry in Faculty of Electrical Engineering. He is responsible lecture in Electric Machines I & II-undergraduate. He now is work as first Lector for course of Dynamics of Electric Machine-graduate

Denis Qirollari received the B. CH. and M.S. degrees in Electrical Engineering from Faculty of Electrical Engineering of Polytechnic of Tirana in 2009 and 2011, respectively. During 2012-2018, he started work as electrical engineer in Transmission System Operator, Department of Panning of Power Systems. During this time he has been involved in many studies related to the development of Albanian Power System He now is work as Senior Planning Engineer at National Grid, US.